9-2007

Ultra Wideband Channel Characterization and Ranging in Data Centers

N. Udar
Southern Illinois University Carbondale

K. Kant
Intel Corporation

R. Viswanathan
Southern Illinois University Carbondale, viswa@engr.siu.edu

D. Cheung
Intel Corporation

Published in Udar, N., Kant, K., Viswanathan, R., & Cheung, D. (2007). Ultra Wideband Channel Characterization and Ranging in Data Centers. IEEE International Conference onUltra-Wideband, 2007(ICUWB 2007), 322-327. doi: 10.1109/ICUWB.2007.4380963

Ultra Wideband Channel Characterization and Ranging in Data Centers

N. Udar†, K. Kant‡, R. Viswanathan†, D. Cheung‡
udarn@siu.edu, viswa@engr.siu.edu, {krishna.kant | david.b.cheung}@intel.com

Abstract—**This paper presents a detailed measurement based characterization of the Ultra Wideband (UWB) channels in a data center environment and examines the accuracy of direct ranging using Time of Arrival (ToA)measurements. Modern data centers present a unique indoor environment that to our knowledge has not yet been characterized. Our ranging experiments indicate that it is possible to achieve an accuracy of fraction of a meter via direct ranging and point to the feasibility of locating individual servers using more sophisticated cooperative ranging.**

Key words: Ultra Wideband (UWB), Wireless USB, data centers, Saleh-Valenzuela channel model, path loss, ranging.

I. Introduction

In recent years, Ultra Wideband (UWB) communications has received great interest from both the research community and industry. UWB transmissions are subject to strict power regulations and thus are best suited for short-range communications. The IEEE standards group on personal area networks (PANs) is actively working on UWB based communications under Wi-Media (previously 802.1.5.3a task group) alliance and 802.15.4a task group. UWB has been adopted as the underlying technology for the Wireless USB (Universal Serial Bus) standard – a wireless replacement for the popular wired USB interface, and also being developed by the Wi-Media.

Although WUSB is designed for the client space, its ubiquity will allow it to be exploited in servers for creating an out-of-band fabric which can be used for a variety of applications in a data center. The objective of this paper is to lay a foundation for a new application scenario for UWB in data center management e.g., asset location. This paper presents a characterization of UWB wireless channel model in data centers via direct measurements and examines the accuracy of ranging using Time of arrival (ToA) technique.

The rest of the paper is organized as follows. In section II we briefly describe some basic concepts of wireless channel characterization and discuss previous work, particularly the IEEE 802.15.4a channel models. In section III we describe our measurement setup, methodology, challenges and results. We also compare data center model against the IEEE 802.15.4a indoor models. In section III-E we apply the data center channel characteristics to the asset location problem in the data center. Finally, in section IV we conclude the paper and discuss future work.

†N. Udar and, R. Viswanathan are with Southern Illinois University, Carbondale, IL. ‡K. Kant and D. Cheung are with Intel Corporation, Hillsboro, OR

Fig. 1. A row of racks in a data center

II. UWB Propagation Models

A. Indoor Channel Characterisitcs

Wireless propagation channels have been investigated extensively in the literature, particularly in the cellular communications context and a large number of channel models are available in the literature. The signal that has propagated through a wireless channel consists of multiple replicas (echoes) of the originally transmitted signal; this phenomenon is known as *multipath propagation*. The different multipath components (MPCs) are characterized by different delays and attenuations. The correct modeling of the parameters describing the MPCs could provide a better understanding of radio propagation in these channels [1]. In this paper, we focus on wideband signals.

With the use of a ultra wideband signal, a channel model that describes the radio propagation in an indoor medium can be described by one of three channel models: tap-delay line Rayleigh fading model used in IEEE 802.11, the Saleh-Valenzuela (S-V) model [2], [3], and the Δ-K model [4]. Based on a detailed set of studies, IEEE 802.15.3a committee settled on a S-V model to enable comparison of various technologies in the WPAN area [6]. The SV model assumes that the MPCs arrive in clusters rather than in continuum and this aspect has been verified using indoor measurements and is shown by our measurements as well. This is a result of the very fine resolution the UWB waveforms provide. In particular, multipath reflections and diffractions from various indoor objects that differ by 0.3 m in traveled distance will arrive at the receiver 1 ns apart.

B. Data Center Environment

A data center can be compared with a library room where we have several metallic racks containing servers. The racks are 78" high, 23-25" wide and 26-30" deep and are generally placed side by side in a row without any spacing (other than a supporting beam). A rack can be filled up with either rack mount or blade servers. Rack mounted servers go horizontally

1-4244-0521-1/07/$20.00 ©2007 IEEE

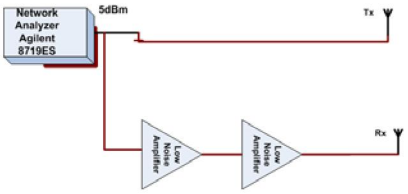

Fig. 2. Experimental Setup for Measurements

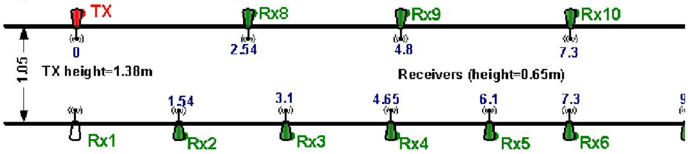

Fig. 3. Locations of transmitter & receivers

in the rack and have typical heights of 1U or 2U where a "U" is approximately 1.8". The high density blade servers go vertically in a 19" high chassis, with 14 blades/chassis. Fig 1 shows a single row of racks with 3U rack-mount servers and some empty slots. If all racks in the data center can be treated as essentially continuous metal blocks, the characterization could be relatively straightforward. The racks are not always filled up with servers, thereby creating many holes through which the radiation can leak. In fact, because of the increasing stress placed by high density servers on cooling and power distribution infrastructure, the racks in older data centers simply cannot be filled to capacity. The net result is a unique environment with "organized clutter".

As stated above, much of the indoor UWB channel characterization work has been on home and office environments. An exception is [5] which provides a characterization of a cluttered industrial environment. Although the environment studied in [5] has a lot of clutter, the clutter does not have any organized pattern. This unorganized clutter can be seen to produce mostly Rayleigh distributed small-scale fading signal, with only a few paths exhibiting Nakagami distributions." This is different from the data center environment, thereby confirming the need for direct measurements in the data center.

C. S-V and Related Propagation Models

802.15.4a (LDR) focuses on low data rate applications ($\leq$ 0.25 Mbps) and is set to serve the specific needs of industrial, residential and medical applications. 802.1.5.3a (HDR) is suitable for high data rate applications that require very high quality of service, for example multimedia applications. LDR is further characterized by very low battery consumption to last for several months to years. Location awareness is a unique characteristic of LDR whereas it is an optional feature in HDR. HDR uses S-V model where ray inter arrival times are modeled as a Poisson process. LDR uses modified S-V model where ray inter arrival times are modeled as a mixed Poisson process.

The Saleh-Valenzuela model [2] assumes that the received signal for a transmitted impulse consists of C clusters, and R_c MPCs (or "rays") within the cth cluster. Let T_c denote the arrival time of cth cluster (i.e., that of the first ray within this cluster) and let τ_{cr} denote the arrival time of the rth ray within the cluster (relative to the arrival time of first ray). Then the

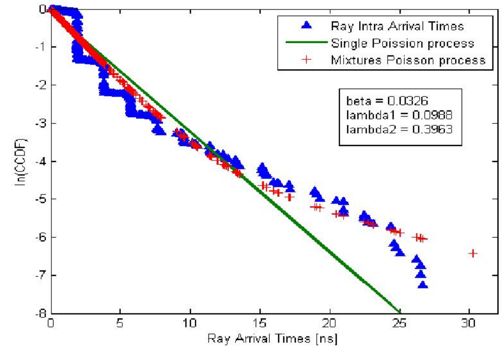

Fig. 4. Ray Inter-arrival Times for S-V Model

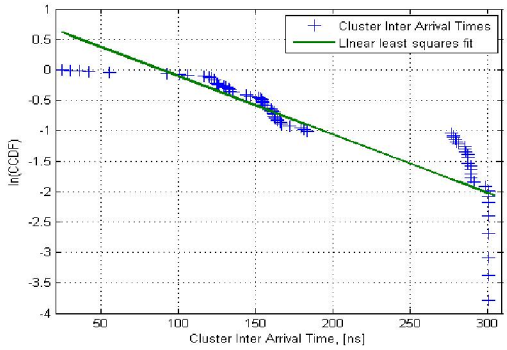

Fig. 5. Cluster Inter-arrival Times for S-V Model

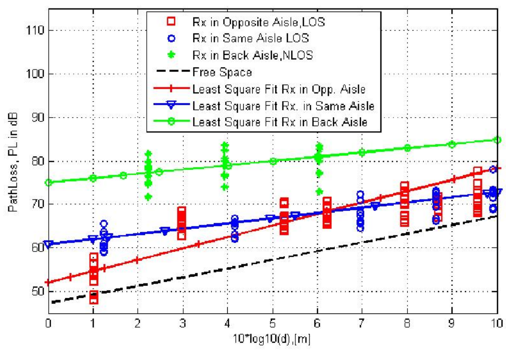

Fig. 6. Pathloss vs. distance from transmitter

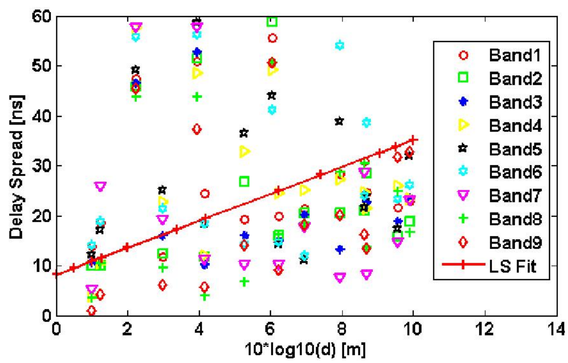

Fig. 7. Delay spread vs. distance from transmitter

impulse response $h(t)$ of the channel is given by:

$$h(t) = \sum_{c=1}^{C} \sum_{r=1}^{R_c} a_{cr} \delta(t - T_c - \tau_{cr}) \quad (1)$$

where $\delta(.)$ is the Dirac delta function, and a_{cr} is the relative weight (or multipath gain coefficient) of ray (c, r).

The basic S-V model assumes that both inter-cluster and inter-ray times are exponentially distributed, thereby making the corresponding processes Poisson. That is,

$$P(T_c - T_{c-1} > x) = e^{-\lambda_c x} \quad (2)$$

$$P(T_{c,r} - T_{c,r-1} > y) = e^{-\lambda_r y} \quad (3)$$

where λ_c and λ_r are, respectively, mean cluster and ray arrival rates. As for the coefficients a_{cr}'s, the S-V model assumes an exponential decay for both cluster power and ray power within a cluster as a function of the delay. That is,

$$a_{cr}^2 = a_{00}^2 e^{-T_c/\Gamma} e^{-\tau_{cr}/\gamma} \quad (4)$$

where a_{00}^2 is the power of the very first ray, and Γ and γ are the cluster and ray decay constants. The a_{00} parameter comes from the path loss model. Reference [3] discusses a modified S-V model where the ray arrival process is modeled as a mixture of two Poisson processes. We shall see later that our data center measurements agree well with this model.

In addition to MPC arrival characterization, there are several other aspects to consider in order to fully describe the channel. One such aspect is the *path loss model*, which indicates how the power decays as a function of distance. For free-space propagation, the path loss at distance d is given by $(4\pi d/\lambda)^2$, where λ is the wavelength. In a cluttered environment, the loss exponent could be significantly different from 2 because of reflection and diffraction. The path loss could vary depending on the location, shape, reflectivity, permittivity, etc. of the clutter and can be regarded as a normal random variable when expressed in dB [7].

Path loss, cluster power decay, and ray decay phenomena discussed above are all deterministic in nature. In reality, there are also small scale random signal variations or *amplitude fading* that must be considered. One way to characterize this is by considering cluster and ray power as a random variable with associated mean and standard deviation. The standard deviations σ_c and σ_r then become essential parameters of the S-V model and need to be estimated. The distribution of the amplitude itself is important and is typically found to be Lognormal, Nakagami or Rayleigh.

The third aspect of interest is *time variance* of the channel. Wireless channel characteristics are influenced by environmental factors such as temperature, humidity, air flow, movements, etc. Fortunately, in data center environments, such variations are expected to be small and infrequent, and time variance characterization may be unnecessary. Our measurements validate this conclusion as shown later.

III. UWB Channel Characterization

A. Measurement Setup

The measurements were conducted in a medium sized data center using an Agilent 8719ES vector network analyzer (VNA), a pair of low noise amplifiers, a pair of discone antennas and cables as shown in Fig. 2. The VNA was set to transmit 1601 continuous waves distributed uniformly over 3-8 GHz. This results in the frequency step of 3.125 MHz which gives maximum excess delay of 320 ns. This frequency range was chosen over 3-8 GHz due to limitation of available power amplifiers and low noise amplifiers. The 5 GHz bandwidth gives a temporal resolution of 0.2 ns.

Antenna calibrations were provided by Intel Corp. in an anechoic chamber to remove the antenna effects in post processing. Measurements were conducted in the Intel data center where the transmitter (Tx) was fixed towards one end of the aisle and multiple positions for the receiver (Rx) were considered. Fig. 3 shows the location of the transmitter and receivers. To measure the small scale statistics of the channel the Rx was moved 25 times around each local point over a 5 by 5 square grid with 5 cm spacing. Each point on the grid is referred as a spatial point. Primarily only line-of-sight scenarios were considered. Three measurements were made in the back aisle which can be considered as non line-of-sight.

B. Post Processing

At each spatial point, the VNA records the overall transfer function, which includes the effect of the channel, amplifiers, attenuators and the cables. The channel transfer function (CTF) is obtained from this after removing the effects of antennas, amplifiers, attenuators and cables from the transfer function. The CTF at each point is transformed into channel impulse response (CIR) using pass band inverse Fourier transform. The CIR'S are then analyzed to obtain various channel parameters.

C. Channel Modeling

The Measurements described in section III-A is used to generate Figs. 4 and 5, which show the plots of complementary cumulative distribution functions of ray inter-arrival times and cluster inter-arrival times, respectively. Fig. 4 also shows the S-V model fit (labeled as single Poisson process), and a mixture of two Poissons, which was proposed as a modified S-V model for the indoor data in [3]. The Poisson mixture is based on the following equation:

$$P(T_{c,r} - T_{c,r-1} > y) = \beta e^{-\lambda_1 y} + (1 - \beta) e^{-\lambda_2 y} \quad (5)$$

where λ_1 and λ_1 are mean ray arrival rates and β is the mixture probability Fig. 4 shows clearly that the modified S-V model provides a better fit to the data than the single Poisson process. For cluster inter-arrival times in Fig. 5, a single Poisson process provides a reasonable fit only if the clusters arriving at times greater than 120 ns are ignored. However, the latter cluster arrivals correspond to multipaths due to reflections from the wall of a data center.

Fig. 6 shows the path loss (PL) in dB versus the distance between different receivers (Rxs) and the transmitter (Txs). Fig. 6 shows that the path loss exponent is less than 2 and is slightly more than 1. That is, the path loss in a data center decreases much slower with distance than in free space. This is due to the fact that a large number of diffractions and reflections taking place in the metallic racks and other

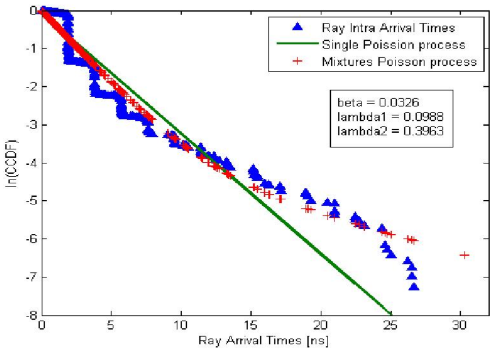

Fig. 8. Regression Fit for Ray Power

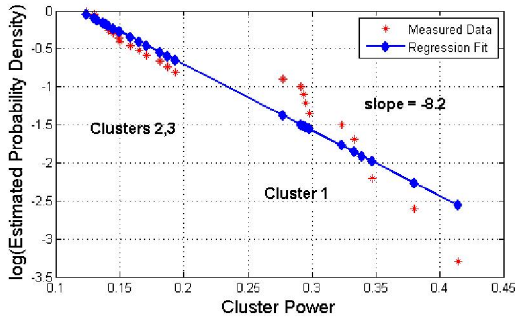

Fig. 9. Regression Fit for Cluster Power: Averaged over bands

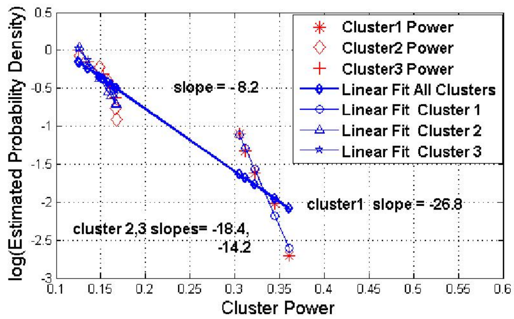

Fig. 10. Regression Fit for Cluster Power: Averaged over locations

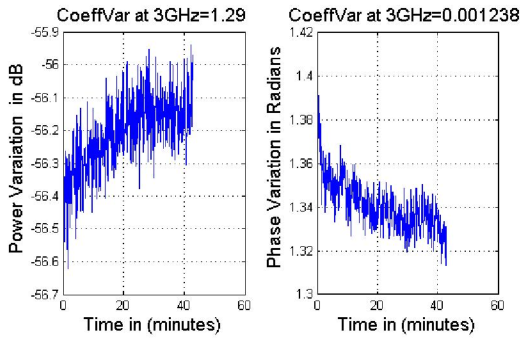

Fig. 11. Time variation of channel characteristics

components present in the vicinity of Tx and Rx contribute to a much increased received power than is possible in free space. Fig. 7 shows the measured delay spread against the distance between the Tx and the Rx. In general, delay spread increases with distance. This means that the Rxs at locations further from the Tx receive multipath signals arriving at small as well as large time separations.

The next parameter of interest is the cluster and ray decay constants Γ and γ introduced in eqn (4). These constants can be determined by plotting the histograms of cluster and ray power as shown in Figs. 8, 9 and 10. As stated earlier, the implicit assumption here is that both cluster and ray power decay exponentially for successive clusters/rays independent of the frequency band used. It is seen from the first two graphs that the fit for exponential decay is quite good for both ray and cluster power. However, as Fig. 10 demonstrates, there is a significant dependence on the WUSB frequency bands in the 3-8 GHz range. We still compute the slope (8.2ns) from the overall regression fit line which is used in Table II to compare this environment against others. However, it is clear that such a regression fit does not model the data well. Therefore, we also do separate regression fits for Cluster1 and Cluster2/3, which can be used to characterize the frequency dependence.

To study the temporal characteristics the channel was measured repeatedly over 43 minute period between 3-8 GHz. The power and Phase variations were obtained from the measurements. Fig. 11 shows one such measurement at 3GHz. It is seen that variations in both power and phase are extremely small and can be ignored for all practical purposes. Strangely, the variations show increasing or decreasing trends over 10s of minutes; however, in all cases the trend flattened out and did not suggest any instability. The major significance of these results is that we may need fewer measurements for ranging purposes within a data center. However, a much more reliable estimation of distances is possible through cooperative measurements.

The final property to consider is the small scale fading shown in Fig. 12. This graph shows a plot of logarithm of probability density of received power scaled up to a normalizing constant. A linear fit indicates that the power distribution is exponential, and hence the amplitude distribution is Rayleigh.

D. *Comparison against other models*

Tables I and II compare channel characteristics of data center environment against other major indoor environments considered by the IEEE 802.15.4a precision ranging group [8]. These include (a) residential environment (small houses, condos, apartments, etc.), (b) office (small rooms & cubicles along with long narrow corridors), and (c) industrial (a lot of clutter). Tables I compares the path loss parameters for the four environments. It is seen that the path loss at 1m distance is considerably higher in both data centers and industrial environments. This is perhaps due to a lot of short-distance metallic clutter in both environments. The path loss exponent beyond 1m for data centers is comparable to indoor office (but not so for industrial environments). The standard deviation of the assumed log-normal *shadowing* (or large scale path loss variation) is also similar to those in other environments. In contrast, the standard deviation is quite large for industrial environments. This difference results from the fact that in a

TABLE I
COMPARISON OF PATH LOSS IN INDOOR ENVIRONMENTS. ‡ INADEQUATE DATA

Parameters	Symbols	Residential		Indoor Office		Industrial		Data Center	
		LoS	NLoS	LoS	NLoS	LoS	NLoS	LoS	NLoS‡
Path Loss at 1 meter	$PL_0[dB]$	43.9	48.7	36.6	48.7	56.7	56.7	55.0	74.7
PL exponent at > 1m	n	1.79	4.58	1.63	3.07	1.2	2.15	1.6	0.91
PL lognormal std at > 1m	$\sigma_S[dB]$	2.22	3.51	1.9	3.9	6.0	6.0	2.1	3.0

TABLE II
COMPARISON OF POWER DELAY PROFILE IN INDOOR ENVIRONMENTS‡ INADEQUATE DATA

Parameters	Symbol	Residential		Indoor Office		Industrial		Data Center	
		LoS	NLoS	LoS	NLoS	LoS	NLoS	LoS	NLoS‡
Mean number of clusters	$\overline{L}$	3.0	3.5	5.4	1.0	4.75	1.0	2.1	3.5
Inter-cluster arrival rate [1/ns]	Λ	0.047	0.12	0.016	NA	0.071	NA	0.016	0.014
Ray1 arrival rate [1/ns]	λ_1	1.54	1.77	0.19	NA	NA	NA	0.068	0.39
Ray2 arrival rate [1/ns]	λ_2	0.15	0.15	2.97	NA	NA	NA	0.380	0.04
First ray component prob.	β	0.95	0.045	0.184	NA	NA	NA	0.029	0.96
Cluster decay constant [ns]	Γ	22.61	26.27	14.6	NA	13.47	NA	8.2	8.2
Ray decay constant [ns]	γ_0	12.53	17.5	6.4	NA	0.651	NA	4.1	4.7

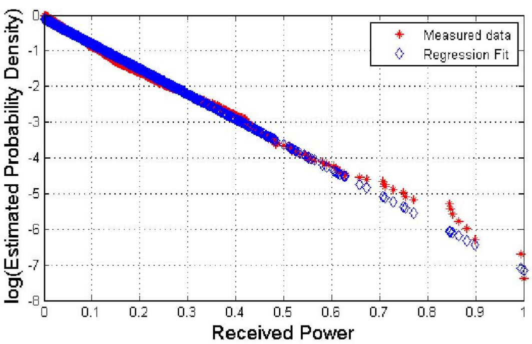

Fig. 12. Regression Fit for Small Scale Power Distribution

data center, longer distance environment is not very different from normal indoor, whereas this is not the case for general industrial environments.

Table II compares the power delay characteristics in the four environments. One interesting observation here is that the number of clusters in the data center is very small – just two in most cases. This again results from the fact that beyond the level of racks, there are no more reflectors or diffractors in this environment. Indeed the cluster decay constant of 8.2ns, which corresponds to about 2.5m distance, indicates that we are unlikely to see many clusters. This is also corroborated by the mean number of clusters of 2.1 within the data center.

E. Ranging in Data Centers

Asset location consists of two sub problems (a) ranging – or estimating distance between a pair of devices, and (b) location determination using a large number of range estimates with a goal to minimize errors (e.g., see [9], [10], [11]). In this paper we concentrate only on (a) and provide some results on achievable ranging accuracy in data centers.

With UWB, range measurement can be made either using RSS (received signal strength) or ToA or a combination of the two (assuming that the WUSB radios are equipped with these capabilities). The accuracy of ToA measurement is complicated by the absence of line of sight (LOS) as well as by the presence of multipath components (briefly termed as non-line-of-sight, NLOS) condition. NLOS leads to a positive bias and a larger variance in the estimated range parameter [11], [12], [10]. ToA measurement error seems to obey Gaussian distribution reasonably well, with a positive mean and a higher variance associated with NLOS as compared to zero mean and a smaller variance associated with LOS (Fig. 5 in [11]). The RSS technique suffers significantly higher errors due to a variety of influences on transmitted and received power. Furthermore, RSS errors tend to be multiplicative (as opposed to additive for ToA) [12]. Nevertheless, RSS based measurements can help weed out outliers in ToA based measurements.

The problem of estimating ranging error in ToA is considered in [13]. The paper models the errors due to multipath as zero mean Gaussian with magnitude proportional to $log(1+d)$. In case of NLOS, the first received signal peak is not the strongest and may not be used for ToA measurement since the measurements usually pick out the strongest received signal. In other words, the bias in distance measurement will have a positive mean. In general, it is not known whether a given received signal falls in LOS or not. Thus, the individual estimations may include both LOS and NLOS (biased) estimates. The subsequent step of doing estimation from collective measurements (not discussed in this paper) can be used to estimate the bias.

Fig. 13-14 show the estimated distances of the Rx's based on the time of arrival (ToA) data and the measured (actual) distances. The raw distance estimate is based on c times the arrival instant of the first ray with significant power, where c is the speed of light. Because of multiple diffractions and reflections encountered in a data center environment, the first ray with significant power could be a multipath signal and not a direct path signal. For each Rx location, 25 different measurements were performed and hence range estimates, in 3 - 8 GHz spectrum, were obtained. Fig. 13 shows the true distances of the Rxs, the mean, the median, and the trimmed mean (mean of the remaining data after throwing out the largest and the smallest observations) of the 25 positions raw

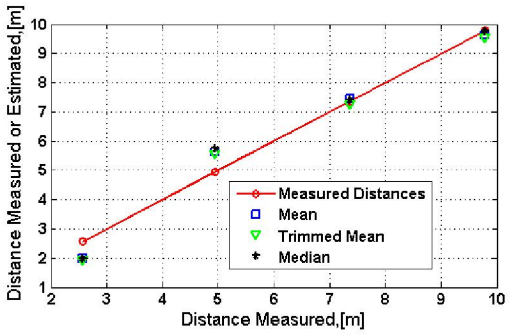

Fig. 13. Range Measurements for receivers in opposite aisle

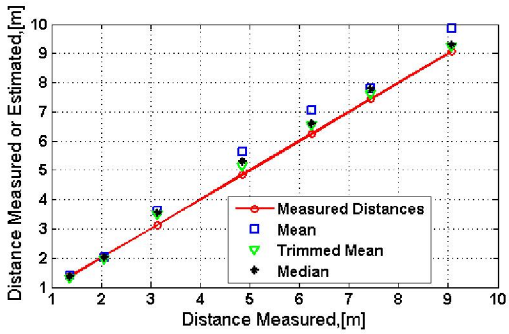

Fig. 14. Range Measurements for receivers in the same aisle

estimates for the receivers in the opposite aisle. Fig. 14 shows results for receivers in same aisle.

TABLE III
RANGE ERROR OF TRIMMED MEAN AT VARIOUS RX LOCATIONS

Opposite recv locn	Ranging error abs	Ranging error %	Same-side recv locn	Ranging error abs	Ranging error %
RX1	0.05	3.70	RX8	0.25	2.56
RX2	0.10	4.85	RX9	0.09	1.33
RX3	0.38	11.3	RX10	0.60	12.10
RX4	0.31	6.40	RX11	0.64	24.80
RX5	0.30	4.80			
RX6	0.30	4.80			
RX7	0.18	2.40			

From these figures, we see that the trimmed mean performs better than mean or median raw estimates in most cases. The absolute error and percentage error based on trimmed mean raw estimates for various Rx locations is shown in table III. The percentage error does not necessarily increase with distance. However, the farthest two receivers in the same aisle show large errors. These errors are dominated by the blockage properties (weaker LOS) at that Rx locations. In case of LOS, the average raw estimate of error is only 4 percent. It is not know if a similar percentage error will hold at smaller distances, however, the results do indicate a fairly decent accuracy from the perspective of locating individual servers. Further measurements coupled with improved estimation algorithms that address NLOS conditions are needed in order to have a reliable asset location mechanism using WUSB radios.

We also made a small number of measurements on the back of the racks primarily to examine how much of the RF signal "leaks" over to the other side. In all cases, it was found that the signal suffered an additional 30-40 dB loss. Consequently, the ranging results on the back side (not shown for brevity) weren't very useful (100% or more errors). It should be noted that such a result is neither surprising nor problematic. With successive racks standing side by side w/o any gaps, it is obvious that not much signal makes it to the back. The result isn't problematic because each row will have its own radios and results can be "chained" together at racks on each end.

IV. DISCUSSION AND FUTURE WORK

In this paper we characterized the UWB propagation within a data center environment via direct measurements over the UWB band in an actual data center. The characterization shows that the data center environment is similar but not identical to other indoor environments that have been studied in the past. We also examined the question of UWB based ranging within data centers and showed the kind of ranging errors one can expect in this environment. To our knowledge, this is the first study of its kinds and lays the ground work for Wireless USB based asset location that we are interested in. The future work on the subject consists of an in depth examination of cooperative ranging within the data center while exploiting the invariant properties of this environment.

Acknowledgements: We are grateful to Mujeeb Mohammed for his help with data analysis.

REFERENCES

[1] R. J. M. Cramer, R. A. Scholtz, and M. Z. Win, "Evaluation of an Ultra-Wide-Band Propagation Channel," IEEE Trans. Antennas and Prop. 50, 2002, pp. 561-570.
[2] A. Saleh and R. Valenzuela, "A Statistical Model for Indoor Multipath Propagation," IEEE JSAC, vol. SAC-5, no. 2, Feb. 1987, pp. 128-137.
[3] C-C Chong, Y. Kim, S-S Lee, "A modified S-V clustering channel model for the UWB indoor residential environment", Proc. of 1st IEEE Veh. Technol. Conf, pp. 58-62, Stockholm, Sweden, May 2005.
[4] H. Hashemi, "Impulse Response Modeling of Indoor Radio Propagation Channels," IEEE JSAC, Vol. 11, No. 7, Sept. 1993, pp.967-978.
[5] J. Karedal, S. Wyne, et. al., "Statistical analysis of the UWB channel in an industrial environment", Vehicular Technology Conf, Vol1, Sept. 2004, pp. 81 - 85.
[6] Molisch, A.F.; et.al "Channel models for ultrawideband personal area networks" ,Wireless Comm., IEEE vol. 10, Dec. 2003 pp. 14 - 21 .
[7] C-C. Chong, Y. Kim, S-S. Lee, "Statistical characterization of the UWB propagation channel in various types of high-rise apartments", 2nd wireless comm. & networking conf, Vol. 2, Mar 2005 pp. 944 - 949.
[8] A.F. Molisch et.al. "IEEE 802.4a Channel Model-Final Report", Nov. 04 Avaliable Online http://www.ieee802.org/15/pub/TG4a.html
[9] J.N. Ash and R.L. Moses, "Outlier compensation in sensor network self-localization via the EM algorithm," IEEE ICASSP, 2005, pp. IV-749-752.
[10] N.S. Correal, S. Kyperountas, et. al., "An UWB relative location system", 2003 IEEE Conference on Ultra Wideband Systems and Technologies, Nov. 2003, pp. 394- 397.
[11] N. Patwari, A.O. Hero, et.al., "Relative estimation in wireless sensor networks," IEEE Trans. Signal Process., pp. 2137-2148, Aug 2003.
[12] N. Patwari, J.N. Ash, et. al., "Locating the nodes- cooperative localization in wireless sensor networks," IEEE Signal Process. Mag., pp. 54-69, July 2005.
[13] B. Alavi and K. Pahlavan, "Modeling of ToA based distance measurement error using UWB indoor radio measurements", IEEE comm. letters, Vol 10, No 4, April 2006, pp. 275-277.
[14] N. Udar, K. Kant, R. Viswanathan, D. Cheung, "Characterization of Ultra wide band channel in data center environments", poster presentation w/ a short summary, to appear in Networking 2007, May 2007.